


 Cite this: *RSC Adv.*, 2022, 12, 26966

 Received 9th September 2022  
 Accepted 13th September 2022

DOI: 10.1039/d2ra05685b

[rsc.li/rsc-advances](https://rsc.li/rsc-advances)

# A gold(I)-catalysed approach towards harmalidine an elusive alkaloid from *Peganum harmala*†

 Solène Miaskiewicz, Jean-Marc Weibel, Patrick Pale  and Aurélien Blanc \*

Upon gold catalysis, the 2,3-dihydropyrrolo[1,2-*a*]indole motif, encountered in few but interesting bioactive natural products, was efficiently obtained from *N*-aryl 2-alkynylazetidide derivatives. In an attempt to apply this methodology to the synthesis of harmalidine, isolated from the seeds of *Peganum harmala*, advanced amino 2,3-hydropyrrolo[1,2-*a*]indol(one) derivatives were readily obtained in only 11 steps from but-3-yn-1-ol. While the reported structure of harmalidine could not be reached from these intermediates, a surprising 12-membered diimino dimer was isolated. Extensive comparison of the reported harmalidine NMR data to the experimental and calculated data of our synthetic molecules, harmaline or the synthesised *N*-methylharmaline show discrepancies with the proposed natural product structure.

## Introduction

Traditional local uses and folk medicine often rely on plant extracts. The latter are a rich source of interesting natural products and numerous bioactive compounds have been isolated as such. The plant *Peganum harmala* (Fig. 1, right), common in semi-arid areas such as Sahara borders, the Middle East, or Central Asia, is a typical example. This plant was used by indigenous people to make a 'magic' beverage, which promotes hallucinogenic and psychoactive effects, but also as a treatment for asthma, diabetes, and rheumatism. Among the compounds identified from this plant, alkaloids named harmine, harmaline, harmalidine, harmalol, harmol and tetrahydroharmine (Fig. 1, top) are mostly responsible for the psychoactive activities. These substances belong to the  $\beta$ -

carboline family, except for harmalidine which contains a 2,3-dihydropyrrolo[1,2-*a*]indole motif (Fig. 1, middle).<sup>1</sup>

Less common than other fused indolo-polycyclic motifs, pyrrolo[1,2-*a*]indole nevertheless represents the core of various interesting natural products. From chinese medicine were isolated isatisine A and some derivatives, including one exhibiting anti-HIV activity.<sup>2</sup> Other pyrrolo[1,2-*a*]indole derivatives have been isolated from plants and used for treating infections, skin lesions, rheumatic pain<sup>3</sup> or exhibiting filaricidal (polysin)<sup>4</sup> or antimalarial (flinderoles)<sup>5</sup> activities (Fig. 2). The pyrrolo[1,2-*a*]indole motif is also the core of a family of antibiotic and anti-cancer compounds named mitomycins A-K (Fig. 2).<sup>6–8</sup> The importance and the variety of pyrrolo[1,2-*a*]indole natural product biological activities have induced several synthetic studies,<sup>9–11</sup> especially in the mitomycin area.<sup>12–14</sup>

Engaged in gold-catalysed cascade reactions,<sup>15</sup> we reasoned that these reactions could provide an alternative and rapid access to pyrrolo[1,2-*a*]indole derivatives (Scheme 1). In 2013, we reported a new route to such compounds based on the gold

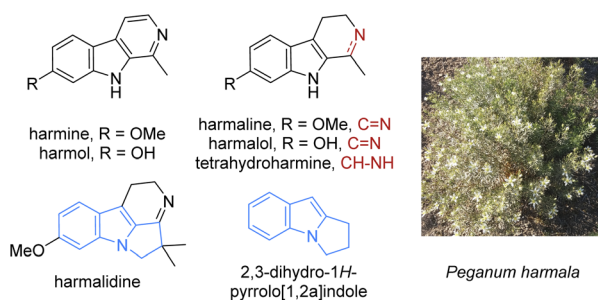


Fig. 1 Main psychoactive harmala alkaloids and harmalidine structure including the 2,3-dihydropyrrolo[1,2-*a*]indole motif.

Laboratoire de Synthèse, Réactivité Organiques et Catalyse, Institut de Chimie, UMR 7177 - CNRS, Université de Strasbourg, 4 Rue Blaise Pascal, 67070 Strasbourg, France. E-mail: [ablanc@unistra.fr](mailto:ablanc@unistra.fr)

† Electronic supplementary information (ESI) available. CCDC 2111055. For ESI and crystallographic data in CIF or other electronic format see <https://doi.org/10.1039/d2ra05685b>

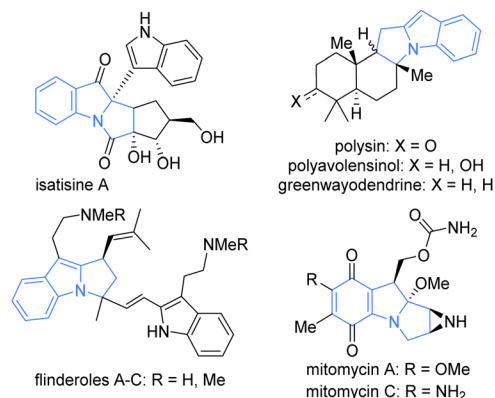


Fig. 2 Natural products exhibiting the pyrrolo[1,2-*a*]indole motif.



catalysed rearrangement of *N*-aryl-2-alkynylazetidines and we demonstrated its efficiency through the formal syntheses of the antibiotic 7-methoxymitosene and of a 5-HT<sub>2C</sub> receptor agonist.<sup>16</sup>

In the present report, we described our effort towards the total synthesis of harmalidine based on this gold-catalysed reaction.

Applying this rearrangement to this context implies to start from the *N*-3-methoxyphenyl azetidine **C**, which should be obtained through the formal [2 + 2] condensation and reduction (Scheme 2).<sup>16,17</sup> This would require the formation of the imine **D** from the aldehyde **F** and 3-methoxyaniline. Isobutyrate ester was selected, as the condensation of its enolate to imine **D** should allow introducing the *gem*-dimethyl unit present in the natural product structure. Upon rearrangement, the resulting product **B** must then be oxidized at a benzylic position to a ketone.<sup>18</sup> The latter would serve for forming the fourth harmalidine cycle through an intramolecular aza-Wittig reaction from the azide **A**.

## Results and discussion

### Synthesis of the key *N*-3-methoxyphenyl azetidine **C**

For convenience, we started the synthesis of **C** from the commercially available butyn-3-ol (Scheme 3). It was first protected as *tert*-butyldimethyl or diphenylsilyl ethers under classical conditions. The so-formed silyl butynyl ethers **1a, b** were then formylated upon alkyne deprotonation and addition of dimethylformamide in THF at low temperature.<sup>16,17</sup> The resulting aldehydes **2a, b** were then converted to imines **3a, b** by condensation with 3-methoxyaniline. The best and most convenient procedure at this stage was achieved by mixing both reagents in the presence of magnesium sulphate in ether at room temperature. The expected imines **3a, b** were pure enough after filtration to be directly engaged in the next step.

Upon addition to a lithium enolate solution derived from ethyl isobutyrate, these imines were efficiently converted to the expected *N*-3-methoxyphenyl *gem*-dimethyl azetidinones **4a, b** in good to high yields. The latter were then reduced to the corresponding azetidines. The best conditions were those described



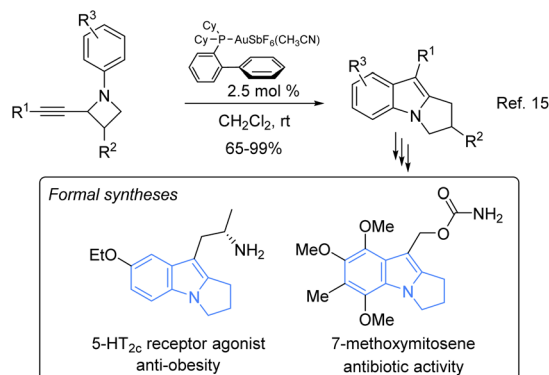
Scheme 2 Our retrosynthesis of harmalidine involving our key gold-catalysed rearrangement of *N*-aryl azetidines to pyrrolo[1,2-*a*]indoles.

by Ojima in the presence of *in situ* formed monochloroalane,<sup>19</sup> providing the expected azetidines **5a, b** (synthon **C**) within seconds in good to high yields, while avoiding opening side-reactions.

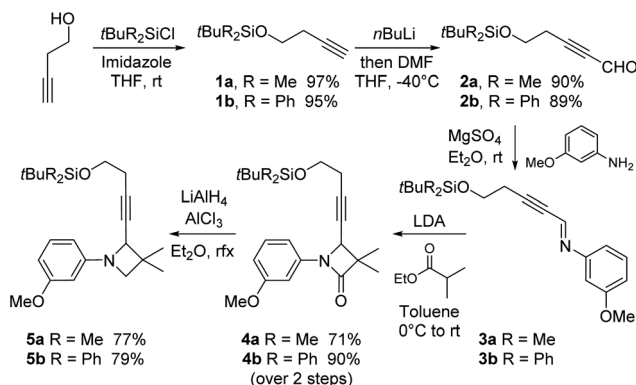
### Gold-catalysed rearrangement: from *N*-3-methoxyphenyl alk-1-ynyl dimethylazetidine **C** to pyrrolo[1,2-*a*]indole **B**

With these azetidines in hand, the gold-catalysed rearrangement was studied. Under our precedent optimized conditions,<sup>16</sup> the expected 2,3-dihydropyrrolo[1,2-*a*]indoles were readily obtained but in modest yields due to some degradation. A brief condition screening revealed that 2-biphenyldicyclohexylphosphino-gold(i) hexafluoroantimonate was still the best catalyst but 1,2-dichloroethane (DCE) turned out to be better as solvent, while refluxing minimized degradation due to short reaction times. Excellent conversions and yields were thus achieved within 2 minutes under such conditions (Scheme 4). Rewardingly, this reaction could be performed in gram scale without compromising reaction time and yields.

As expected from an azetidine carrying on its nitrogen atom a 3-substituted phenyl group, two regioisomers were formed from both substrates **5a** and **5b**, but they were easily isolated by flash chromatography, respectively providing **6a** (47%)/**7a** (43%) and **6b** (53%)/**7b** (38%). Interestingly, the size of the alkynyl substituent seemed to play a favourable role in the corresponding regioselectivity. While an almost 1 : 1 ratio was observed starting

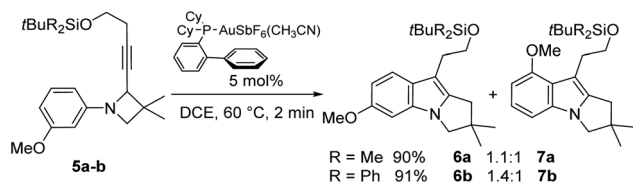


Scheme 1 Rearrangement of *N*-aryl-2-alkynylazetidines catalysed by gold and its application to formal syntheses.



Scheme 3 Synthesis of the key intermediate *N*-aryl azetidines.





Scheme 4 The gold-catalysed rearrangement of *N*-aryl azetidines to pyrrolo[1,2-*a*]indoles.

from the *tert*-butyldimethylsilyl substituted **5a**, a slightly higher selectivity was achieved with the bulkier *tert*-butyldiphenylsilyl derivative **5b** in favour of the desired regioisomer. It is worth noting that a similar effect of bulkiness on regioselectivity has already been observed in our preliminary studies.<sup>16</sup>

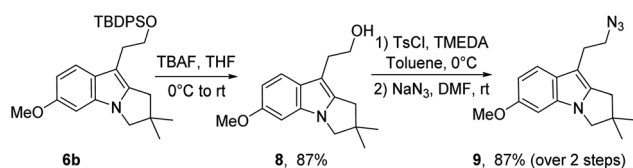
### Functional modifications of intermediate B

To advance towards the third key step of the proposed strategy, *i.e.* the intramolecular aza-Wittig reaction, the *O*-silylated pyrrolo[1,2-*a*]indole **6b** must be converted to the azido derivative and the 2 $\alpha$  position of the 2,3-dihydropyrrolo[1,2-*a*]indole motif must be selectively oxidised.

The latter required specific conditions, which will be discussed in the next section. The former was readily achieved by a conventional desilylation, *O*-tosylation and azido substitution sequence (Scheme 5). It is nevertheless worth noting that the tosylation step required specific base and conditions to avoid direct *in situ* chlorination and degradation.

The selective oxidation at the 2 $\alpha$  position of the 2,3-dihydropyrrolo[1,2-*a*]indole moiety proved much more tricky than expected. To study this critical step and set up appropriate conditions, the hexyl substituted 2,3-dihydropyrrolo[1,2-*a*]indole model compound **6c** (Table 1: R = H, Fn = C<sub>4</sub>H<sub>9</sub>) was synthesized using the same strategy described in Schemes 3 and 4 (See ESI†).

Applying to our model **6c** the modified sulfoxide-based oxidation method (DPSO/TFAA) of indoles 2 $\alpha$  position reported by Kawasaki *et al.*<sup>20</sup> selectively afforded the alcohol **10a** although in modest yield (entry 1). Therefore, the reaction conditions were adjusted by using DMSO, as less hindered sulfoxide than DPSO, leading efficiently within short time to ketone **11a** (entry 2). Unfortunately, DMSO/TFAA oxidation conditions were deleterious with the more functionalized substrates **6a**, **b** or **9** (Entry 3). Nevertheless, the alcohol **10b** could be selectively formed from silylated compound **6b** in the presence of triethylamine as base (entry 4). Shifting to Swern conditions (DMSO/(COCl)<sub>2</sub>/Et<sub>3</sub>N), the reaction gave a mixture of



Scheme 5 Functional group interchange of pyrrolo[1,2-*a*]indole **6**.

alcohol **10c** and ketone **11c** starting from the silylated compound **7b** (entry 5). It is worth noticing that the alcohols **10** could not be correctly oxidised to the corresponding ketone in independent reactions with various reagents. However, such conditions were ineffective on azido derivative **9** as the starting material remain untouched (entry 6). Rewardingly, the formation of the expected azido ketone **11d** was observed in very good yield without addition of base (entry 7).

### Staudinger and aza-Wittig reactions

As first shown by Staudinger, azides can be converted to iminophosphoranes upon treatment with phosphine. After work-up, iminophosphoranes are hydrolysed to the corresponding amine and phosphine oxide.<sup>21</sup> However, without water, iminophosphoranes could react with aldehydes or ketones, forming azaphosphetane intermediates, which decompose to imine and phosphine oxide, in a process analogue to the Wittig reaction.<sup>22</sup>

With the azido 2,3-dihydropyrrolo[1,2-*a*]indolone **11d**, such a sequence should directly provide the expected natural product (Scheme 6). However, and despite extensive investigation, no harmalidine could be detected whatever the conditions with different phosphines, including supported ones,<sup>23</sup> and only the corresponding amine could be isolated, although in low to modest yields. These results revealed that the iminophosphorane intermediate was formed but could not react with the neighbouring ketone to form the azaphosphetane [2 + 2] intermediate.

To solve this problem, we envisaged producing this amine by adjusting the Staudinger conditions to form the expected imine in a second step. The former could only be achieved by using the combination of a non-hindered and nucleophilic phosphine, *i.e.* the simple trimethylphosphine, with a mildly basic aqueous solution. Under these conditions, the amino 2,3-dihydropyrrolo[1,2-*a*]indolone **12** was isolated in good yield (Scheme 7). The structure of this compound was confirmed by X-ray diffraction of suitable crystals, grown after HPLC purification (see ESI†).‡

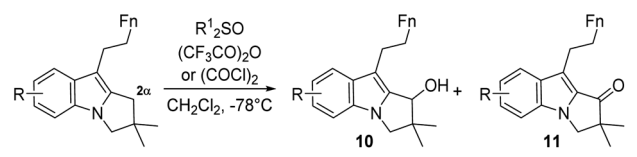
The intramolecular cyclisation of this amino ketone was then attempted. However, and despite extensive experimentation (see Table 2 for selected examples), none of the expected cyclised product was detected. Either no transformation (*e.g.* entries 1–3) or extensive degradation (*e.g.* entries 4–5) was observed. Under a few conditions, an imine was isolated (entry 6), but its spectroscopic analysis, notably HR-MS, revealed a dimeric structure ascribed to the 12-membered diimino macrocycle **13** (see Table 2 Scheme). Attempts to avoid this dimerization were undertaken under higher dilution conditions, but only returned the starting material unchanged (entry 7).

It is interesting to note here that the NMR spectra of this dimer **13** did not fit with the data reported for the harmalidine natural product, although both were quite similar (see below).

These results as well as the aza-Wittig results may be due to the hindrance brought by the *gem*-dimethyl groups adjacent to

‡ Crystallographic data for **12** have been deposited in the CCDC under accession number 2111055.



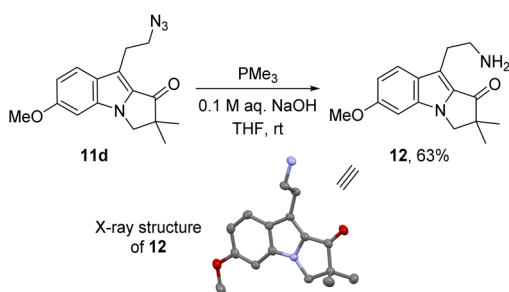
Table 1 Benzylic oxidation of 2,3-dihydropyrrolo[1,2-*a*]indole at the 2 $\alpha$  position


entry	Substrate	Reagents (equiv.)	Base	Time(min)	Alcohol 10 (%)	Ketone 11 (%)
1	<b>6c<sup>a</sup></b> , R = H Fn = C <sub>4</sub> H <sub>9</sub>	DPSO (3) TFAA (3)	—	45	27 ( <b>10a</b> )	—
2	"	DMSO (3) TFAA (3)	—	1	Trace	88 ( <b>11a</b> )
3	<b>6a, b or 9</b>	"	—	1	Degradation	—
4	<b>6b</b>	DMSO (6) TFAA (3)	NEt <sub>3</sub> (3)	60	64 ( <b>10b</b> )	—
5	<b>7b</b>	DMSO (6) (COCl) <sub>2</sub> (3)	NEt <sub>3</sub> (6)	15	60 ( <b>10c</b> )	29 ( <b>11c</b> )
6	<b>9</b>	"	NEt <sub>3</sub> (6)	120	No reaction	—
7	"	"	—	15	—	87 ( <b>11d</b> )

<sup>a</sup> The model compound **6c** was prepared according to the same gold catalysed strategy, see ESI. DPSO = diphenylsulfoxide. TFAA = trifluoroacetic anhydride.



Scheme 6 The expected Staudinger-aza-Wittig reaction towards harmalidine, highlighting the iminophosphorane and azaphosphetane intermediates.



Scheme 7 Formation of the amino pyrrolo[1,2-*a*]indolone **12** by a Staudinger reaction and its ellipsoid representation (hydrogen atoms have been omitted for clarity).

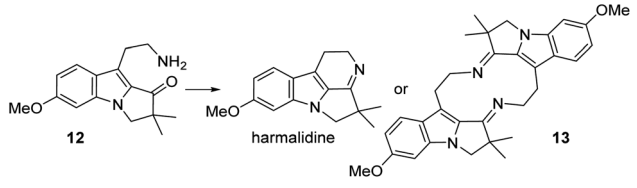
the carbonyl group in **11d** or **12**. From the iminophosphorane derived from **11d**, the [2 + 2] transition state towards the azaphosphetane intermediate may be too difficult to reach due to strong steric interaction with the *gem*-dimethyl groups, especially with large substituents around the phosphorous atom (Scheme 6). For the intramolecular imine formation from **12**,

the Bürgi-Dunitz angle required for the amine nucleophilic addition to the carbonyl group may be hampered again by this *gem*-dimethyl groups, but also by the strain induced by the rigidity of the 2,3-dihydropyrrolo[1,2-*a*]indolone motif. The latter effect would favour inter- rather than intra-molecular condensation, although the former would also be slowed down by the *gem*-dimethyl groups; and indeed, it took up to 6 days to get 55% yield of **13** (entry 6 in Table 2).

In response to this problematic imine formation, we envisaged a reverse cyclisation strategy *via* substitution of a leaving group at the terminal carbon side chain position by the nitrogen atom of an amine at the 2 $\alpha$  position of the 2,3-dihydropyrrolo[1,2-*a*]indole moiety (Scheme 8, top). As amine can be directly introduced by oxy-amination at the 2 $\alpha$  position (see below), cyclisation and deprotection would provide the reduced form of harmalidine, mentioned in the original discovery report.<sup>1</sup> For this approach, we had to synthesized the chloroethyl 2,3-dihydropyrrolo[1,2-*a*]indole derivative **6d** from azetidione **5a**, because the introduction of halogenated group using classical methods from **8** consistently led to the formation of large amount of degradation products. The chlorinated but sensitive derivative **6d** was finally available in 4 steps: TBDPS deprotection, tosylation, Finkelstein-type reaction and our gold-catalysed rearrangement (Scheme 8, bottom).

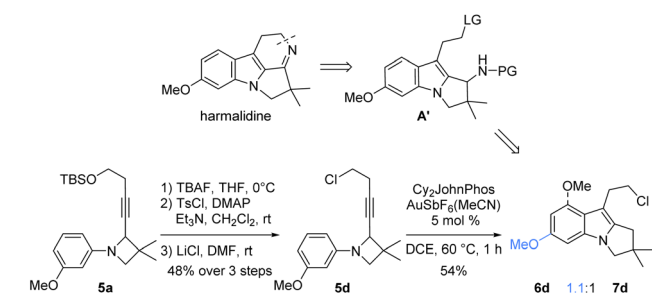
The direct amination of the 2 $\alpha$  position of **6d** was performed using modified conditions of the oxidation reaction developed above (Table 1). In the presence of DMSO and oxalic chloride (1 equivalent each) and an excess of the desired amine, amination could occur (Table 3). From the silylated substrate **6b**, the expected aminated 2,3-dihydropyrrolo[1,2-*a*]indole **14** derivatives could be obtained in high yield with benzylamine (**14a**, 78%), but in modest yield with allylamine (**14b**, 25%) together with degradation products for the latter (entry 1 vs. 2). Unfortunately, starting from the sensitive chloro compound **6d**, the reaction



Table 2 Imine formation from the amino pyrrolo[1,2-*a*]indolone **13**


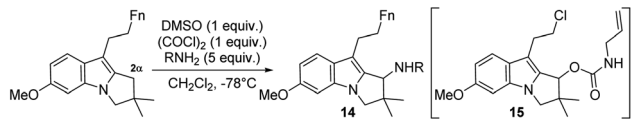
Entry	Reagent	Solvent	Conc. (mmol L <sup>-1</sup> )	Time (h)	Product
1	MS 4A	THF, rt	10	24	– <sup>a,b</sup>
2	NH <sub>4</sub> Cl	EtOH, 70 °C	4	48	– <sup>a,b</sup>
3	ArCOO.NEt <sub>3</sub> H	Tol, 70 °C	10	24	– <sup>a,b</sup>
4	TiCl <sub>4</sub>	THF, rt	10	24	Degradation
5	Ti(OiPr) <sub>4</sub>	THF, 80 °C	0.2	24	Degradation
6	cat. PPTS	PhH, 120 °C	10	144	Dimer <sup>b</sup> ( <b>13</b> ) 55% – <sup>a,b</sup>
7	cat. PPTS	PhH, 120 °C	0.2	168	– <sup>a,b</sup>

<sup>a</sup> No reaction. <sup>b</sup> Starting material recovered. MS: molecular sieves; PPTS: pyridinium *para*-toluenesulfonate.



Scheme 8 Preparation of pyrrolo[1,2-*a*]indole **6d** for reverse cyclisation strategy.

Table 3 Direct amination of 2,3-dihydropyrrolo[1,2-*a*]indole at the 2 $\alpha$  position



Entry	Substrate	RNH <sub>2</sub>	Time (min)	Yield (%)
1	<b>6b</b> (Fn = OTBDPS)	Benzylamine	30	78 <sup>a</sup> ( <b>14a</b> )
2	<b>6b</b>	Allylamine	120	25 <sup>b</sup> ( <b>14b</b> )
3	<b>6d</b> (Fn = Cl)	Benzylamine	30	– <sup>c</sup>
4	<b>6d</b>	Allylamine	120	20 <sup>b</sup> ( <b>15</b> )

<sup>a</sup> Isolated along with 18% of remaining starting material. <sup>b</sup> isolated along with unidentified degradation products and starting material. <sup>c</sup> Degradation occurs.

with benzylamine only provided degradation products (entry 3), while with allylamine, another 2,3-dihydropyrrolo[1,2-*a*]indole unexpected derivative **15** was obtained, with a modest yield of 20% (entry 3 vs. 4). Extensive NMR investigation revealed that

an *N*-allylcarbamate group was introduced at the 2 $\alpha$  position, presumably *via* the formation of the corresponding alcohol derivative **10** (see Table 1). Attempts to advance **14a** to a halogenated and/or cyclised intermediate only led to degradation. These results unfortunately precluded the full exploration of the envisaged reverse cyclisation strategy.

### Surprises in NMR spectra

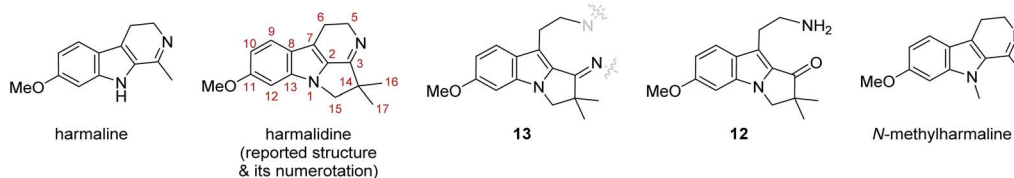
The present results raised questions about the structure reported for the isolated harmalidine natural product. Besides the problems associated to the intramolecular imine formation, differences were observed between the reported data and NMR data gained from our advanced intermediates **11d** or **12** and the obtained dimer **13**. Moreover, harmalidine has never been isolated again despite several studies on alkaloids extracts from *Peganum harmala*,<sup>24</sup> nor synthesized.

The harmalidine structure was mostly assigned by comparison with the harmaline structure, especially for attributing the methoxy position, while the position of the *gem*-dimethyl groups was assigned based on NMR spectra after catalytic hydrogenation of the natural product.<sup>1</sup> However, the <sup>1</sup>H and <sup>13</sup>C NMR comparison was realised in two different deuterated solvents, *i.e.* DMSO-*d*<sub>6</sub> and CDCl<sub>3</sub> for respectively harmaline and harmalidine. To get a better comparison, and as harmaline is commercially available, we got it and recorded its NMR data in CDCl<sub>3</sub> and checked its structure.

When these NMR data were compared to those of the advanced intermediates **11d** and **12**, the dimer **13**, or harmaline in CDCl<sub>3</sub>, some discrepancies clearly showed up (Table 4). Indeed, the methoxyphenyl signals of the natural product were reported as a doublet of doublet at 6.80 ppm (1H, *J* = 8.9 and 1.8 Hz) and two doublets at 7.08 (1H, *J* = 1.8 Hz) and 7.42 ppm (1H, *J* = 8.9 Hz) attributed to H-10, H-12 and H-9, respectively.<sup>1</sup> However, the aromatic AMX spin system for compounds **11d**, **12** or the dimer **13** as well as for harmaline exhibited shielded H-12



**Table 4**  $^1\text{H}$  and  $^{13}\text{C}$  NMR data in  $\text{CDCl}_3$ : reported for harmalidine,<sup>1</sup> and experimental for harmaline, pyrrolo[1,2-*a*]indole **13**, pyrrolo[1,2-*a*]indolone **12** and *N*-methylharmaline



Position	Harmaline		Harmalidine <sup>1</sup>		<b>13</b>		<b>12</b>		<i>N</i> -Methylharmaline	
	$^1\text{H}^a$	$^{13}\text{C}^a$	$^1\text{H}^b$	$^{13}\text{C}^b$	$^1\text{H}$	$^{13}\text{C}$	$^1\text{H}$	$^{13}\text{C}$	$^1\text{H}$	$^{13}\text{C}$
1 (NH)	8.03 br s	—	—	—	—	—	—	—	—	—
2	—	128.4	—	126.3	—	129.5	—	130.8	—	125.6
3	—	157.0	—	161.3 <sup>c</sup>	—	168.4	—	198.1 (CO)	—	162.3
5	3.83 m	48.2	3.93 t	42.8	4.26 m	56.1	3.09 t	43.2	3.64 t	49.8
6	2.82 m	19.5	3.11 t	19.0	3.41 dd	28.2	3.01 t	28.9	3.01 t	20.7
7	—	117.1	—	119.1	—	109.7	—	116.1	—	118.9
8	—	120.0	—	126.7 <sup>d</sup>	—	126.8	—	126.7	—	118.2
9	7.47 d	120.8	7.42 d	122.1	7.78 d	122.0	7.59 d	123.1	7.43 d	120.9
10	6.83 dd	111.0	6.80 dd	115.0	6.84 dd	111.3	6.81 dd	113.0	6.80 dd	111.0
11	—	158.2	—	144.5 <sup>c</sup>	—	158.0	—	159.0	—	158.4
12	6.86 d	94.5	7.08 d	94.0	6.69 d	91.6	6.67 d	91.7	6.74 d	92.4
13	—	137.4	—	124.4 <sup>d</sup>	—	134.2	—	136.1	—	140.1
14	2.33 s	22.0	—	39.7	—	48.6	—	54.4	3.11 s	34.1
15	—	—	3.30 m	43.0	3.95 s	53.9	4.06 s	50.1	4.07 s	31.2
16	—	—	1.30 s	27.0	1.42 s	27.2	1.36 s	24.9	—	—
17	—	—	1.30 s	14.0	1.42 s	27.2	1.36 s	24.9	—	—
OMe	3.86 s	55.6	3.85 s	55.2	3.89 s	55.6	3.86	55.6	3.89 s	55.5

<sup>a</sup> Chemical shifts obtained from commercially available harmaline. <sup>b</sup> NMR data from ref. 1. <sup>c</sup> Values may be reversed. <sup>d</sup> Values may be reversed.

signals ranging from 6.86 to 6.67 ppm. Similarly, the methylene protons H-15 were reported as a multiplet at 3.30 ppm, while these protons appeared as singlet shifted at 4.09 in **12** and 3.95 ppm in **13**.

The analysis of the harmalidine  $^{13}\text{C}$  NMR data also revealed some inconsistencies. While the  $^{13}\text{C}$  NMR shifts for C-9, C-10 and C-12 are in agreement with those of various 6-methoxy pyrrolo[1,2-*a*]indole derivatives, the reported chemical shifts assigned to C-11 (C-OMe,  $\delta_{\text{C}}$  144.5 or 161.3 ppm) and C-13 (C-N,  $\delta_{\text{C}}$  124.4 or 126.7 ppm) are out of range compared to those of compounds **12**, **13** or harmaline (Table 4) with  $\delta_{\text{C}}$  values between 158 and 159 ppm and between 134 and 137 ppm respectively. Of note, if the  $\delta_{\text{C}}$  161.3 is attributed to C-11 and thus closer to the range, the remaining value  $\delta_{\text{C}}$  144.5 ppm would be assigned to the C-3 imine function but seems rather low compared to harmaline ( $\delta_{\text{C}}$  157.0 ppm) or **13** ( $\delta_{\text{C}}$  168.4 ppm). Furthermore, two different values were reported for the *gem*-dimethyl of the hydroxyprolyl part of the harmalidine ( $\delta_{\text{C}}$  14.0 and 27 ppm), while they seem to exhibit a single signal in  $^1\text{H}$  NMR. It is worth noting that one of these values is very similar to the one measured for dimer **13** ( $\delta_{\text{C}}$  27.0 vs. 27.2 ppm) and close to the *N*-indolic methyl of *N*-methyl harmaline ( $\delta_{\text{C}}$  31.2 ppm).

For further comparison, we prepared the *N*-methyl harmaline since it could be a structural alternative to the postulated harmalidine structure. To get this closely related compound, we

modified the commercially available harmaline by methylation of the indolic nitrogen using iodomethane and NaH as base in DMF (See ESI<sup>†</sup>). Comparison of the  $^1\text{H}$  and  $^{13}\text{C}$  NMR data of *N*-methylharmaline<sup>25</sup> showed again a shielded H-12 signal at 6.74 ppm compared to the reported value for harmalidine and a *N*-methyl signal at 4.07 ppm (H-15) in the same range of H-15 methylene of **12** and **13** (3.95–4.06 ppm). Furthermore, the C-3 imine is again different ( $\delta_{\text{C}}$  162.3 ppm) and closer to those of harmaline or **13** than to the reported harmalidine structure (see above).

These inconsistencies prompted us to compare experimental  $^{13}\text{C}$  NMR data of harmalidine and synthetic compound **13** with  $^{13}\text{C}$  predictions of harmalidine generated by computational chemistry (See Table S1 in ESI<sup>†</sup>). Indeed, computational prediction of NMR spectroscopic data have been used for both structure elucidation of new natural products and structural revisions.<sup>26</sup> Nowadays, user-friendly accessible softwares are available and can be used to evaluate the quality of published  $^{13}\text{C}$  NMR.<sup>27</sup> Based on the difference of experimental and values from Neural Network and HOSE-code  $^{13}\text{C}$  predictions,<sup>28</sup> the same discrepancies were noticed for harmalidine (Table S1 in ESI<sup>†</sup>). Indeed, the major  $\delta_{\text{C}}$  variations was localised on the *gem*-dimethyl hydroxyprolyl part of the harmalidine and on its aromatic C13, while the dimer **13** was in very good agreement with the harmalidine predicted values.



Nevertheless, a significant variation seems to occur at the methylene carrying the non-indolic nitrogen atom (position 5 in harmalidine numbering). This difference is lower in *N*-methyl harmaline ( $\delta_{\text{C}}$  49.8 vs. 42.8 ppm in the reported harmalidine structure), but the two methyl groups are now quite different ( $\delta_{\text{C}}$  31.3 and 34.1 vs. 14.3 and 27.0 ppm). Both *N*-methyl harmaline and the dimeric structure of **13** may thus not correspond to the actual harmalidine structure, despite the nice fit between experimental and calculated NMR values.

Noteworthy, the original isolation paper<sup>1</sup> suggested another chemical structure for harmalidine, mostly from biosynthetic hypothesis. This proposed structure corresponds to an isomer in which the dimethyl groups are located at C-15 position instead of C-14. This proposal was nevertheless excluded upon mass analysis. <sup>13</sup>C predictions of this isomer generated by computational chemistry was also in agreement with this conclusion (See Table S2 in ESI†). Therefore, the exact structure of this natural product remains so far elusive.

## Conclusions

In this work, we demonstrated that our gold catalysed rearrangement of *N*-aryl-2-alkynylazetidines to pyrrolo[1,2-*a*]indoles could be extended to complex substrates and scale up to gram quantities. The synthesis of the psychoactive harmalidine was selected to illustrate the potential of this method. Although advanced amino 2,3-hydropyrrolo[1,2-*a*]indole or indolone intermediates could be readily obtained according to two routes in only 11 steps from but-3-yn-1-ol (14% overall yield), the natural product as reported could not be formed, but a dimeric compound was isolated. The latter exhibits an unusual pyrrolo[1,2-*a*]indole structure involved in a novel 12-membered diimino macrocycle. This structure and various NMR discrepancies between the reported natural structure and those gained through this work suggest revising the proposed structure but do not allow to conclude on the real natural product structure.

Further work is currently underway to re-isolate harmalidine and reinvestigate its structure.

## Author contributions

Solène Miaskiewicz: Investigation Jean-Marc Weibel: validation Patrick Pale: writing – original draft Aurélien Blanc: supervision, writing – review & editing, visualization.

## Conflicts of interest

There are no conflicts to declare.

## Acknowledgements

We gratefully acknowledge the French Ministry of Research and the CNRS for financial support. S. M. thanks the French Ministry of Research for a PhD fellowship. The authors thank Dr Pierre de Frémont for crystallographic structure refinement of compound **12**. The MCAT company is also acknowledged for providing gold catalyst precursors (<https://www.mcat.de>).

## Notes and references

- S. Siddiqui, O. Y. Khan, B. S. Siddiqui and S. Faizi, Harmalidine, a  $\beta$ -Carboline Alkaloid from *Peganum harmala*, *Phytochemistry*, 1987, **26**, 1548.
- J.-F. Liu, Z.-Y. Jiang, R.-R. Wang, Y.-T. Zheng, J.-J. Chen, X.-M. Zhang and Y.-B. Ma, Isatisine A, a Novel Alkaloid with an Unprecedented Skeleton from Leaves of *Isatis indigotica*, *Org. Lett.*, 2007, **9**, 4127.
- (a) D. A. Okorie, Polyavolinamide, an Indolosesquiterpene Alkaloid from *Polyalthia suaveolens*, *Phytochemistry*, 1981, **20**, 2575; (b) C. M. Hasan, T. M. Healey, P. G. Waterman and C. H. Schwalbe, Chemical Studies on the Annonaceae. Part 9. Indolosesquiterpene and Aporphine Alkaloids from *Greenwayodendron* (*Polyalthia*) *suaveolens* Stem Bark. X-ray Crystal Structure of *Greenwayodendrin-3-one*, *J. Chem. Soc., Perkin Trans.*, 1982, **1**, 2807.
- (a) I. Ngantchou, B. Nyasse, C. Denier, C. Blonski, V. Hannaert and B. Schneider, Antitrypanosomal Alkaloids from *Polyalthia suaveolens* (Annonaceae): Their Effects on Three Selected Glycolytic Enzymes of *Trypanosoma Brucei*, *Bioorg. Med. Chem. Lett.*, 2010, **20**, 3495; (b) J. L. Poussett, A. Cave, A. Chiaroni and C. Riche, A novel Bis-indole Alkaloid. X-ray Crystal Structure Determination of Borreverine and its Rearrangement Product on Deacetylation, *J. Chem. Soc., Chem. Commun.*, 1977, 261.
- L. S. Fernandez, M. S. Buchanan, A. R. Carroll, Y. J. Feng, R. J. Quinn, V. M. Avery and A.-C. Flinderoles, Antimalarial Bis-indole Alkaloids from *Flindersia* Species, *Org. Lett.*, 2009, **11**, 329.
- For a review, see: J.-C. Andrez, Mitomycins Syntheses: A Recent Update, *Beilstein J. Org. Chem.*, 2009, **5**, 33, DOI: [10.3762/bjoc.5.33](https://doi.org/10.3762/bjoc.5.33).
- (a) S. Wakaki, H. Marumo, K. Tomioka, G. Shimizu, E. Kato, H. Kamada, S. Kudo and Y. Fujimoto, Isolation of new Fractions of Antitumor Mitomycins, *Antibiot. Chemother.*, 1958, **8**, 228; (b) V. Lefemine, M. Dann, F. Barbatschi, W. K. Hausmann, V. Zbinovsky, P. Monnikendam, J. Adam and N. Bohonos, Isolation and Characterization of Mitomycin and other Antibiotics Produced by *Streptomyces Verticillatus*, *J. Am. Chem. Soc.*, 1962, **84**, 3184; (c) A. Tulinsky, Structure of Mitomycin A, *J. Am. Chem. Soc.*, 1962, **84**, 3188.
- (a) W. T. Bradner, Mitomycin C: A Clinical Update, *Cancer Treat. Rev.*, 2001, **27**, 35, ; For the initially proposed but now proven mode of action, see: (b) V. N. Oyer and W. Szybalski, Mitomycins and Porfiromycin; Chemical Mechanism of Activation and Cross-linking of DNA, *Science*, 1964, **145**, 55.
- For reviews on the synthesis of pyrrolo[1,2-*a*]indoles, see: (a) N. Monakhova, S. Ryabova and V. Makarov, Synthesis and Some Biological Properties of Pyrrolo[1,2-*a*]indoles, *J. Heterocycl. Chem.*, 2016, **53**, 685; (b) Y. G. Shelke, P. E. Hande and S. J. Gharpure, Recent Advances in the Synthesis of Pyrrolo[1,2-*a*]indoles and their Derivatives, *Org. Biomol. Chem.*, 2021, **19**, 7544.



- 10 A. Karadeolian and M. A. Kerr, Total Synthesis of (+)-Isatisine A, *J. Org. Chem.*, 2010, **75**, 6830.
- 11 (a) D. H. Dethe, R. D. Erande and A. Ranjan, Biomimetic Total Syntheses of Flinderoles B and C, *J. Am. Chem. Soc.*, 2011, **133**, 2864; (b) R. M. Zeldin and F. D. Toste, Synthesis of Flinderoles B and C by a Gold-Catalyzed Allene Hydroarylation, *Chem. Sci.*, 2011, **2**, 1706.
- 12 For leading references on mitomycin synthetic studies as well as total syntheses, see: (a) H. Namiki, S. Chamberland, D. A. Gubler and R. M. Williams, Synthetic and Biosynthetic Studies on FR900482 and Mitomycin C: An Efficient and Stereoselective Hydroxymethylation of an Advanced Benzazocane Intermediate, *Org. Lett.*, 2007, **9**, 5341; (b) A. L. Williams, J. M. Srinivasan and J. N. Johnston, Synthesis of an Advanced Intermediate en Route to the Mitomycin Natural Products, *Org. Lett.*, 2006, **8**, 6047; (c) R. S. Coleman, F.-X. Felpin and W. Chen, Mitomycin Synthetic Studies: Stereocontrolled and Convergent Synthesis of a Fully Elaborated Aziridinomitosane, *J. Org. Chem.*, 2004, **69**, 7309; (d) S. J. Danishefsky and J. M. Schkeryantz, *Chemical Explorations Driven by an Enchantment with Mitomycinoids - A Twenty Year Account*, Synlett, 1995, p. 475; (e) T. Fukuyama and L. Yang, Practical total synthesis of ( $\pm$ )-mitomycin C, *J. Am. Chem. Soc.*, 1989, **111**, 8303; (f) T. Fukuyama, F. Nakatsubo, A. J. Cocuzza and Y. Kishi, Synthetic Studies toward Mitomycins. III. Total Syntheses of Mitomycins A and C, *Tetrahedron Lett.*, 1977, 4295.
- 13 R. Peters, P. Waldmeier and A. Joncour, Efficient Synthesis of a 5-HT<sub>2C</sub> Receptor Agonist Precursor, *Org. Proc. Res. Dev.*, 2005, **9**, 508.
- 14 (a) J. S. Webb, D. B. Cosulich, J. H. Mowat, J. B. Patrick, R. W. Broschard, W. E. Meyer, R. P. Williams, C. F. Wolf, W. Fulmor, C. Pidacks and J. E. Lancaster, Structures of Mitomycins A, B, and C and Porfiromycin. Part I, *J. Am. Chem. Soc.*, 1962, **84**, 3185; (b) J. S. Webb, D. B. Cosulich, J. H. Mowat, J. B. Patrick, R. W. Broschard, W. E. Meyer, R. P. Williams, C. F. Wolf, W. Fulmor, C. Pidacks and J. E. Lancaster, Structures of Mitomycins A, B, and C and Porfiromycin. Part II, *J. Am. Chem. Soc.*, 1962, **84**, 3187.
- 15 (a) R. Pertschi, S. Miaskiewicz, N. Kern, J.-M. Weibel, P. Pale and A. Blanc, Gold(I)-Catalyzed Divergent and Diastereoselective Synthesis of Azepines by Ammonium/Ring-Expansion Reactions, *Chem. Catal.*, 2021, **1**, 129; (b) F. Sirindil, S. Golling, R. Lamare, J.-M. Weibel, P. Pale and A. Blanc, Synthesis of Indolizine and Pyrrolo[1,2-a]azepine Derivatives via a Gold(I)-Catalyzed Three-Step Cascade, *Org. Lett.*, 2019, **21**, 8997; (c) F. Sirindil, J.-M. Weibel, P. Pale and A. Blanc, Total Synthesis of Rhazinilam through Gold-Catalyzed Cycloisomerization-Sulfonyl Migration and Palladium-Catalyzed Suzuki-Miyaura Coupling of Pyrrolyl Sulfonates, *Org. Lett.*, 2019, **21**, 5542; (d) R. Pertschi, J.-M. Weibel, P. Pale and A. Blanc, Benzosultam Synthesis by Gold(I)-Catalyzed Ammonium Formation/Nucleophilic Substitution, *Org. Lett.*, 2019, **21**, 5616; (e) S. Miaskiewicz, B. Gaillard, N. Kern, J.-M. Weibel, P. Pale and A. Blanc, Gold(I)-Catalyzed N-Desulfonylative Amination versus N-to-O 1,5-Sulfonyl Migration: A Versatile Approach to 1-Azabicycloalkanes, *Angew. Chem., Int. Ed.*, 2016, **55**, 9088; (f) M. Hoffmann, J.-M. Weibel, P. de Fremont, P. Pale and A. Blanc, Gold(I)/(III)-Catalyzed Rearrangement of Divinyl Ketones and Acyloxyalkynyloxiranes into Cyclopentenones, *Org. Lett.*, 2014, **16**, 908.
- 16 N. Kern, M. Hoffmann, A. Blanc, J.-M. Weibel and P. Pale, Gold(I)-Catalyzed Rearrangement of N-Aryl 2-Alkynylazetidines to Pyrrolo[1,2-a]indoles, *Org. Lett.*, 2013, **15**, 836.
- 17 M. Journet, D. Cai, L. M. DiMichele and R. D. Larsen, Highly Efficient Synthesis of  $\alpha,\beta$ -Acetylenic Aldehydes from Terminal Alkynes using DMF as the Formylating Reagent, *Tetrahedron Lett.*, 1998, **39**, 6427.
- 18 A. Nakamura and M. Nakada, Allylic Oxidations in Natural Product Synthesis, *Synthesis*, 2013, **45**, 1421.
- 19 M. Yamashita and I. Ojima, Effective Route to Azetidines from Azetidin-2-ones with the Use of Hydroalanes as Specific Reducing Agents, *J. Am. Chem. Soc.*, 1983, **105**, 6339.
- 20 (a) M. Tayu, K. Higuchi, M. Inaba and T. Kawasaki, Sulfoxide-TFAA and Nucleophile Combination as new Reagent for Aliphatic C-H Functionalization at Indole 2 $\alpha$ -position, *Org. Biomol. Chem.*, 2013, **11**, 496; (b) K. Higuchi, M. Tayu and T. Kawasaki, Active Thionium Species Mediated Functionalization at the 2 $\alpha$ -Position of Indole Derivatives, *Chem. Commun.*, 2011, **47**, 6728.
- 21 H. Staudinger and J. Meyer, Ueber neue Organische Phosphorverbindungen II. Phosphazine, *Helv. Chim. Acta*, 1919, **2**, 635.
- 22 F. Palacios, C. Alonso, D. Aparicio, G. Rubiales and J. M. de los Santos, The aza-Wittig reaction. An Efficient Tool for the Construction of Carbon-Nitrogen Double Bonds, *Tetrahedron*, 2007, **63**, 523.
- 23 (a) J. Kim and R. J. Thomson, Enantioselective Total Synthesis of the Osteoclastogenesis Inhibitor (+)-Symbioimine, *Angew. Chem., Int. Ed.*, 2007, **46**, 3104; (b) S. Ayesa, B. Samuelson and B. Classon, A One-Pot, Solid-Phase Synthesis of Secondary Amines from Reactive Alkyl Halides and an Alkyl Azide, *Synlett*, 2008, 97.
- 24 For recent examples, see: (a) Z.-N. Wu, N.-H. Chen, Q. Tang, S. Chen, Z.-C. Zhan, Y.-B. Zhang, G.-C. Wang, Y.-L. Li and W.-C. Ye,  $\beta$ -Carboline Alkaloids from the Seeds of Peganum harmala and Their Anti-HSV-2 Virus Activities, *Org. Lett.*, 2020, **22**, 7310; (b) K.-B. Wang, D.-H. Li, Y. Bao, F. Cao, W.-J. Wang, C. Lin, W. Bin, J. Bai, Y.-H. Pei, Y.-K. Jing, D. Yang, Z.-L. Li and H.-M. Hua, Structurally Diverse Alkaloids from the Seeds of Peganum harmala, *J. Nat. Prod.*, 2017, **80**, 551.
- 25 R. N. Gupta and I. D. Spenser, 3,4-Dihydro- $\beta$ -carbolines: I. The Alkylation of 1-Substituted N $\beta$ -Alkyl-3,4-Dihydro- $\beta$ -carbolines Anhydro Bases, *Can. J. Chem.*, 1962, **40**, 2041.
- 26 B. K. Chhetri, S. Lavoie, A. M. Sweeney-Jones and J. Kubanek, Recent Trends in the Structural Revision of Natural Products, *Nat. Prod. Rep.*, 2018, **35**, 514.
- 27 (a) E. Jonas, S. Kuhn and N. Schlörer, Prediction of Chemical Shift in NMR: A Review, *Magn. Reson. Chem.*, 2021, DOI:





**10.1002/mrc.5234**; (b) W. Robien, ed. A. D. Kinghorn, H. Falk, S. Gibbons and J. Kobayashi, Springer International Publishing AG, 2017, pp. 137–215, Ch. 3.A *Critical Evaluation of the Quality of Published <sup>13</sup>C NMR Data in*

*Natural Product Chemistry in Progress in the Chemistry of Organic Natural Products* 105.  
28 N. Haider and W. Robien, <https://nmrpredict.orc.univie.ac.at/c13robot/robot.php>.

